

UNSTEADY AERODYNAMIC FORCES MEASURED ON A FLUTTERING PROFILE

V. Vlček^{*}, I. Zolotarev^{*}, J. Kozánek^{*}

Abstract: The evaluations of optical measurements of the flow field near the fluttering profile NACA0015 with two-degrees of freedom are presented. Mach number of the airflow was $M = 0.21$ and $M = 0.45$, the boundaries of the flutter occurrence. Aerodynamic forces acting on the profile were evaluated in the drag and lift components which enabled to obtain independently the forces corresponding to the upper and lower surfaces of the profile. Using the mentioned decomposition, the new information about mechanism of flutter properties was obtained. The force effects on the upper and lower surfaces are in opposite phases and they are partially eliminated as a result of the circulation around the profile. The cycle changes of this forces cause the permanent energy contribution from the airflow to the vibrating system.

Keywords: Aeroelastic experiments, self-excited vibrations, fluttering profile, wind tunnel.

1. Introduction

The detailed arrangement of the experiment is shown in Vlček et al. (2013). The flow field near the vibrating NACA0015 profile was visualized by the interferometry in the flutter regime. Interferograms were recorded by the high-speed camera using 1000 frames/sec. During the flutter, the profile, as two degrees of freedom dynamic system, oscillated by the coupled translational and rotational motion with large amplitudes. Two cases (the experiment No 2663-02, $M = 0.21$, $Re = 0.25 \cdot 10^6$ and the experiment No 2663-05, $M = 0.45$, $Re = 0.54 \cdot 10^6$) were evaluated. The eigenfrequencies of this system corresponding to zero flow velocity were 19.0 Hz (translation) and 21.5 Hz (rotation). In flutter regime, the flutter frequencies were 21.6 Hz ($M = 0.21$) and 32.3 Hz ($M = 0.45$).

Schematic configuration of experimental model is depicted in Fig. 1. Profile NACA0015 with the chord length 61 mm was used. The axis of rotation was situated in 1/3 of the chord, measured from the leading edge.

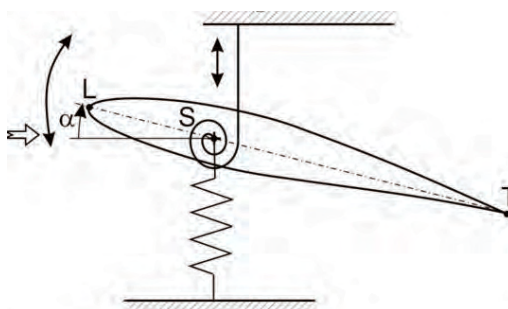


Fig. 1 Schematic configuration of the experiment.

^{*} Ing. Václav Vlček, CSc., Ing. Igor Zolotarev, CSc., Ing. Jan Kozánek, CSc., Institute of Thermomechanics, v.v.i., Academy of Sciences of the Czech Republic, Dolejškova 5, 182 00, Prague 8, Czech Republic, tel.: +420.266053402, fax: +420.286584695, e-mail: vlcek@it.cas.cz

2. Experimental results

The experimental results, discussed in this paper, are based on the evaluation of the interferograms of the non-stationary flow field in the vicinity of the self-excited profile. We suppose the isentropic flow in the evaluation of the interferograms. This simplification was compensated by the possibility of the evaluation of the forces acting separately on different parts of profile surfaces, in this case divided on the upper and lower surfaces.

2.1. Optical measurements

The self-excited vibrations studied here at the Mach numbers 0.21 and 0.45, the ranges of the angles of attack were $\pm 30^\circ$ and $\pm 40^\circ$, respectively. From the whole collection of obtained interferograms two examples (selected in positions with extreme angles of attack, corresponding to the interferogram No 23 and interferogram No 16 of the second measurement) are presented in Fig. 2.

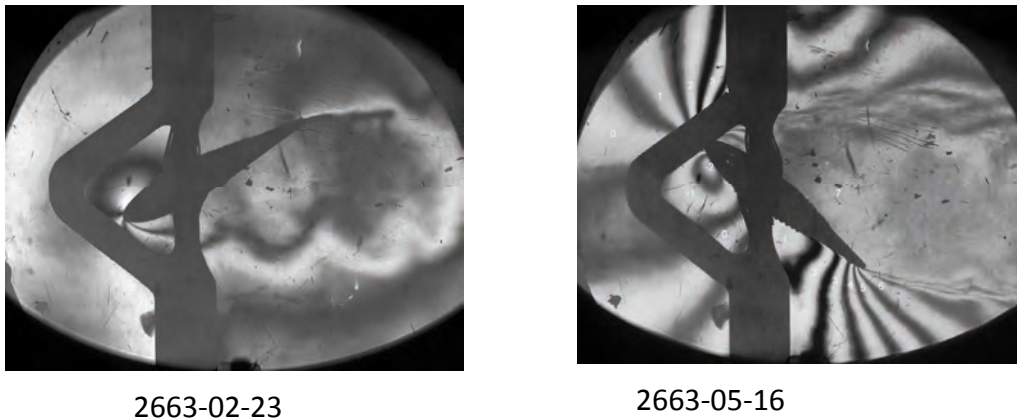


Fig. 2a Interferogram for $M = 0.21$, $\alpha = -30^\circ$. Fig. 2b Interferogram for $M = 0.45$, $\alpha = 40^\circ$.

2.2. The kinematics of the profile

The kinematics of the profile motion was evaluated from the interferograms in discrete time steps 1 ms. The profile translation was considered as the vertical motion of the center of the profile rotation. As the example, the translation and the angle of attack during one period for $M = 0.21$ and $M = 0.45$ is presented in Fig. 3, respectively. In the first case the angle of attack precedes the translation of about 9 ms, on the contrary, in the second one the translation precedes the angle of attack of about 6 ms.

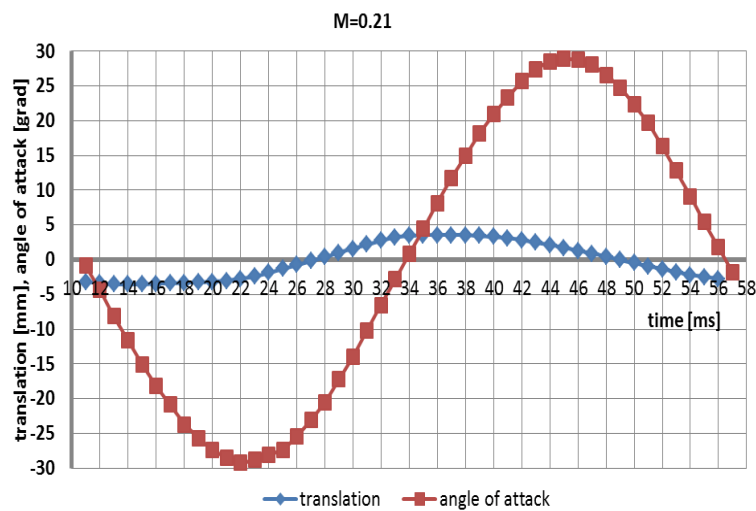


Fig. 3a Translation and angle of attack during one oscillation period, $M = 0.21$.

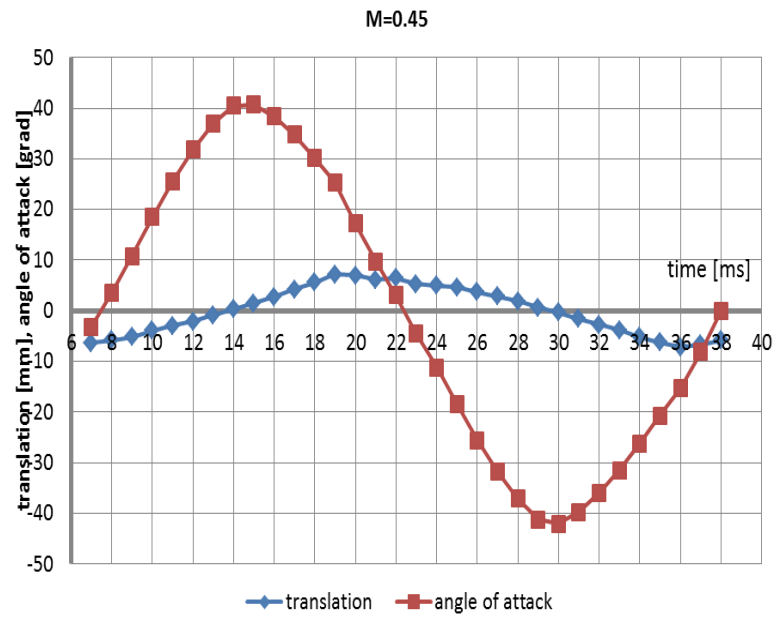


Fig. 3b Translation and angle of attack during one oscillation period, $M = 0.45$.

A summary presentation of the individual positions of the profile during one oscillation period is in Fig. 4. The case $M = 0.21$ (Fig. 4a) is characterized by a small translation trajectory relatively to the angle of attack, on contrary, in the case $M = 0.45$ the translation is greater and the highlighted profile positions with zero angle of attack are farther away, see Fig. 4b.

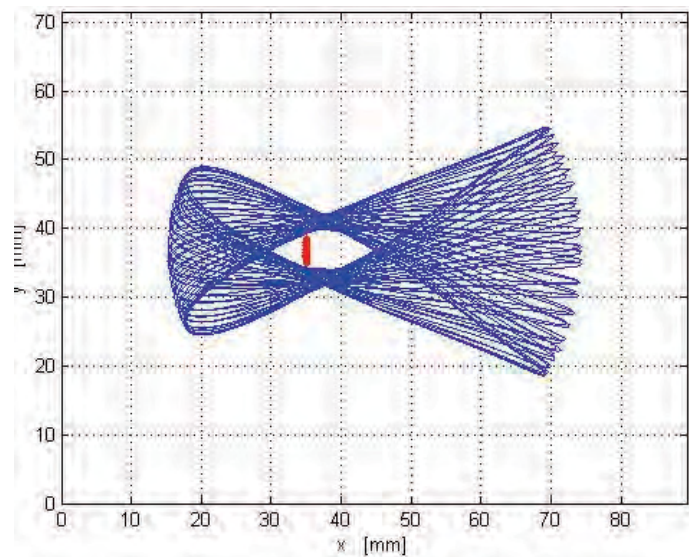


Fig. 4a Profile positions during one period of flutter ($M=0.21$).

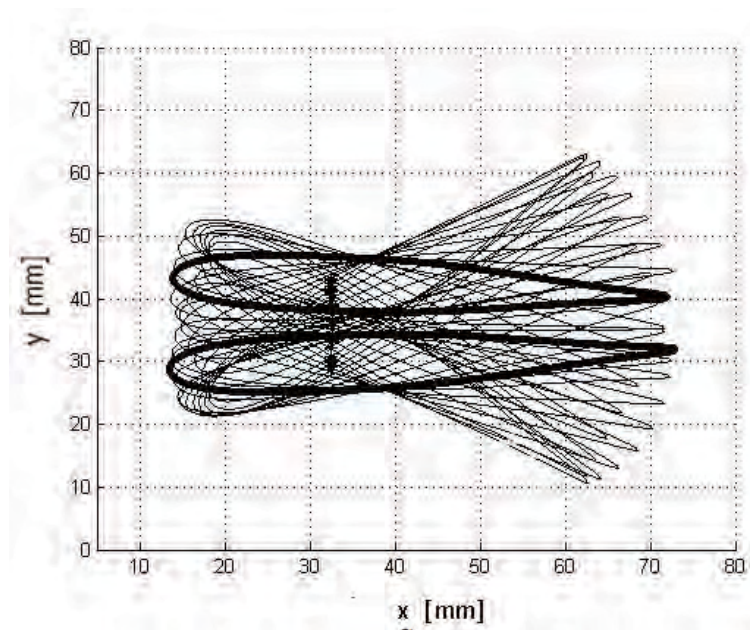


Fig. 4b Profile positions during one period of flutter ($M=0.45$).

Translation of the centre of profile rotation as the function of the angle of attack during one period of flutter are depicted in Fig. 5a and Fig. 5b for the cases $M = 0.21$ and $M = 0.45$, respectively. The different behaviour of the system is also well observable from Fig. 5b, where both cases are depicted in the same scale. The numbers of interferograms meaning simultaneously the time evolution in ms unit, are added for better illustration, beside the measured points.

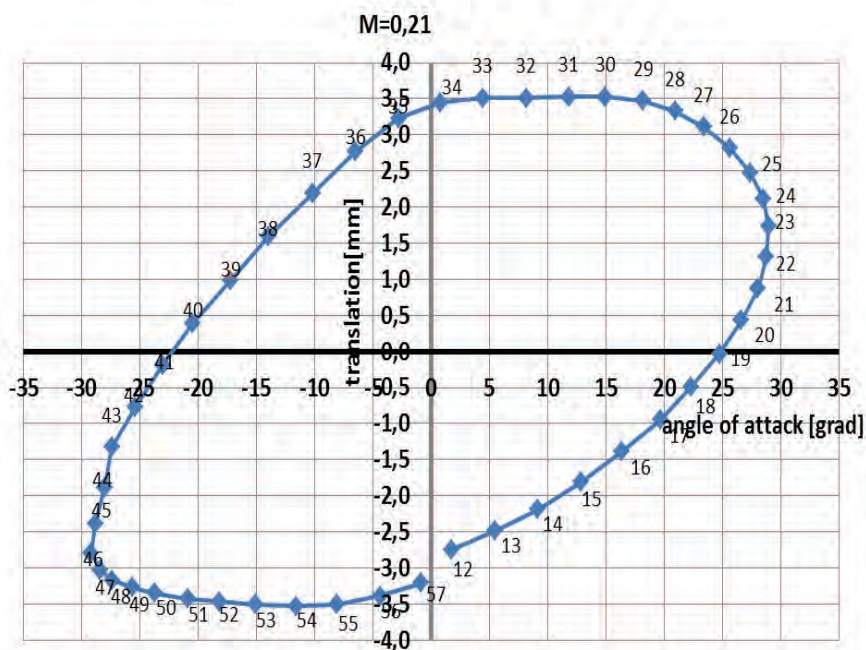


Fig. 5a Translation as the function of the angle of attack during one period of flutter ($M = 0.21$).

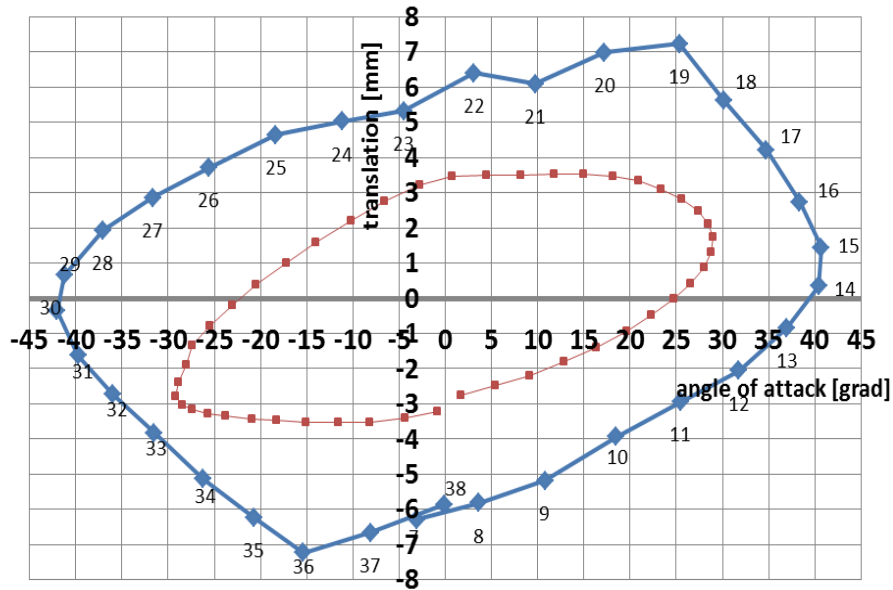


Fig. 5b Translation as the function of the angle of attack during one period of flutter ($M = 0.45$), inner curved line represents the case $M = 0.21$ from Fig. 5a for a comparison.

2.3. The forces acting on the profile

The starting point for the experimental determination of the unsteady aerodynamic forces acting on fluttering profile from the air flow field was in our case the evaluation of the force distribution around the profile surface at discrete time instants during one oscillation period. Here, two cases with different Mach numbers are presented. The one flutter period was evaluated for $M = 0.21$ and for $M = 0.45$ with the help of the 45 and 31 interferograms, respectively. The frequency of the fluttering profile was in the first case 21.6 Hz and 32.3 Hz in second one. The working frequency of the recording by the high-speed camera was 1000 frames/s.

At the beginning of the evaluation process the pressure distribution around the profile surface was obtained as we can see, as an example, in Fig. 6a ($M = 0.21$) and Fig. 6b ($M = 0.45$). The results depicted in Fig. 6 correspond to the one time instant during the vibration period of the flutter state. The complete evaluation of the whole flutter periods are summarized in the Fig. 7 (Fig 7a – $M = 0.21$, Fig. 7b – $M = 0.45$), where P_y is the total lift force, P_{yd} is the lift force acting on the lower surface and P_{yh} is the lift force acting on the upper surface.

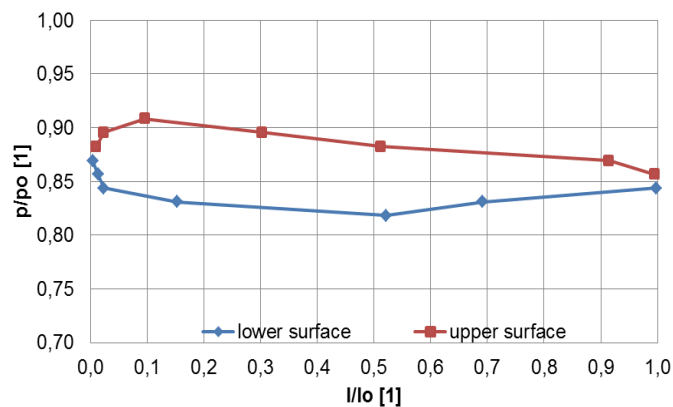


Fig. 6a Pressure distribution on the profile surface ($M = 0.21$) for interferogram from Fig. 2a.

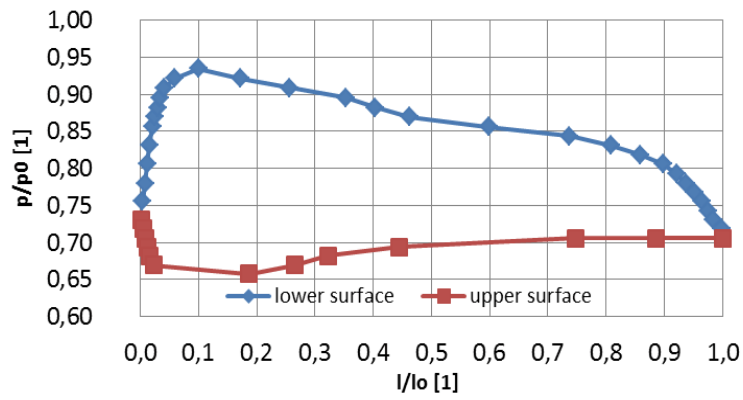


Fig. 6b Pressure distribution on the profile surface ($M = 0.45$) for interferogram from Fig. 2b.

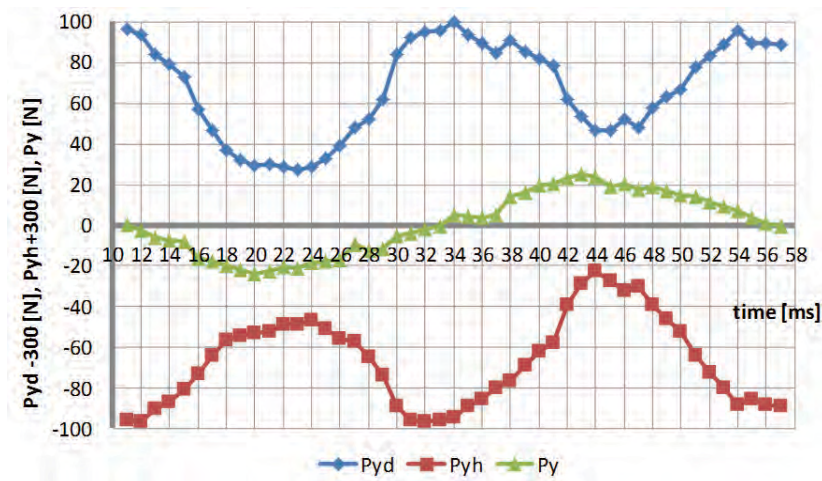


Fig. 7a Total lift force P_y and components acting on lower profile surface P_{yd} and upper surface P_{yh} as a function of time ($M = 0.21$).

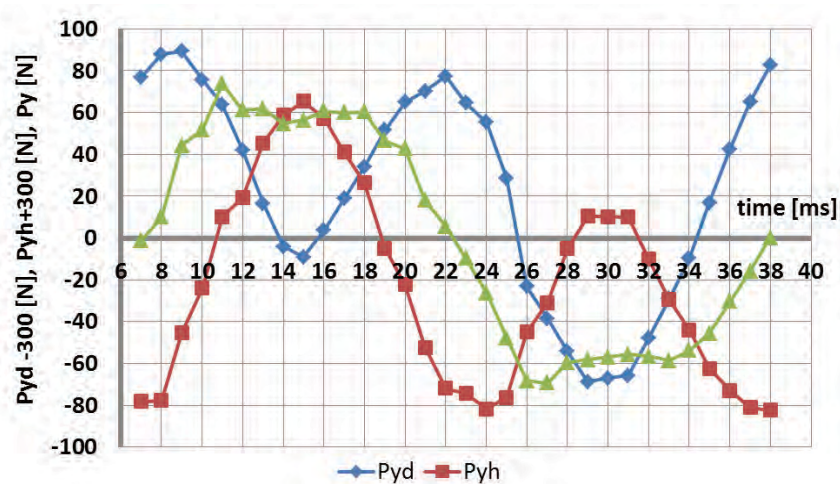


Fig. 7b Total lift force P_y and components acting on lower profile surface P_{yd} and upper surface P_{yh} as a function of time ($M = 0.45$).

For understanding of the energy flow from surrounding airflow to the vibrating structure it is useful to study the relations between the lift forces and the profile movement. The area enclosed by the curved line in Fig. 8 is proportional to the energy obtained from lift forces. For example, as an approximate estimation, from Fig. 8b follows, that the average power supplied to the vibrating profile from the flow is about 50 W.

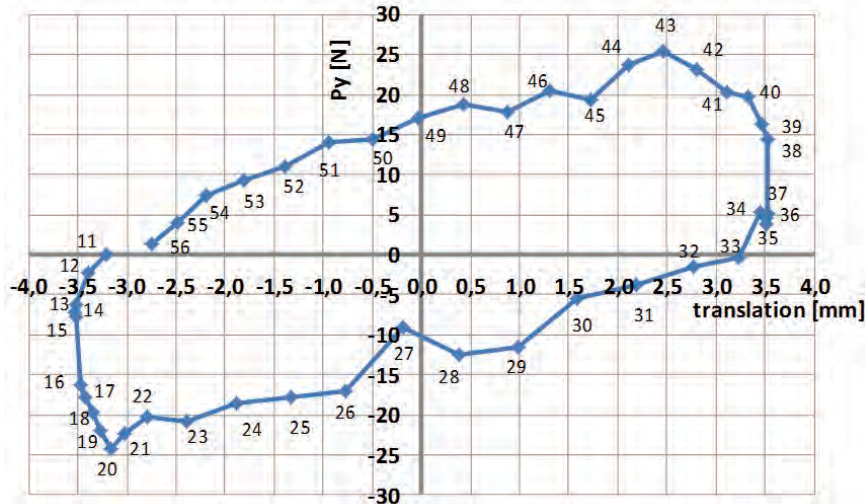


Fig. 8a Total lifting force as a function of profile translation ($M = 0.21$).

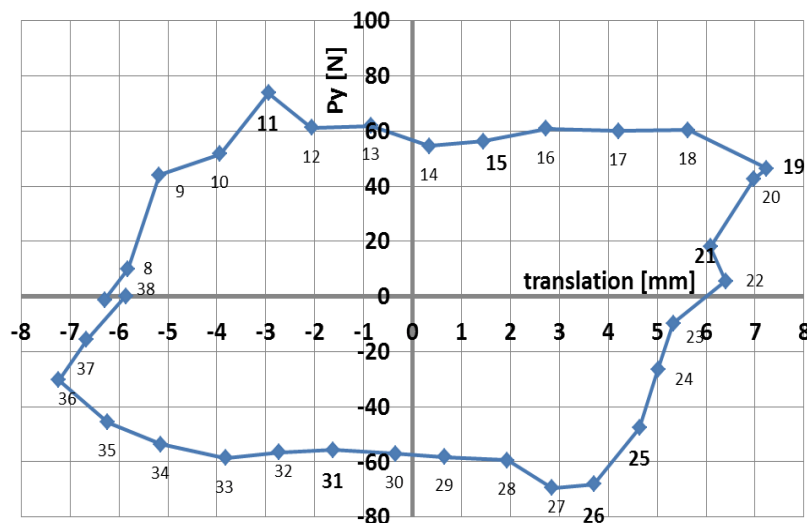


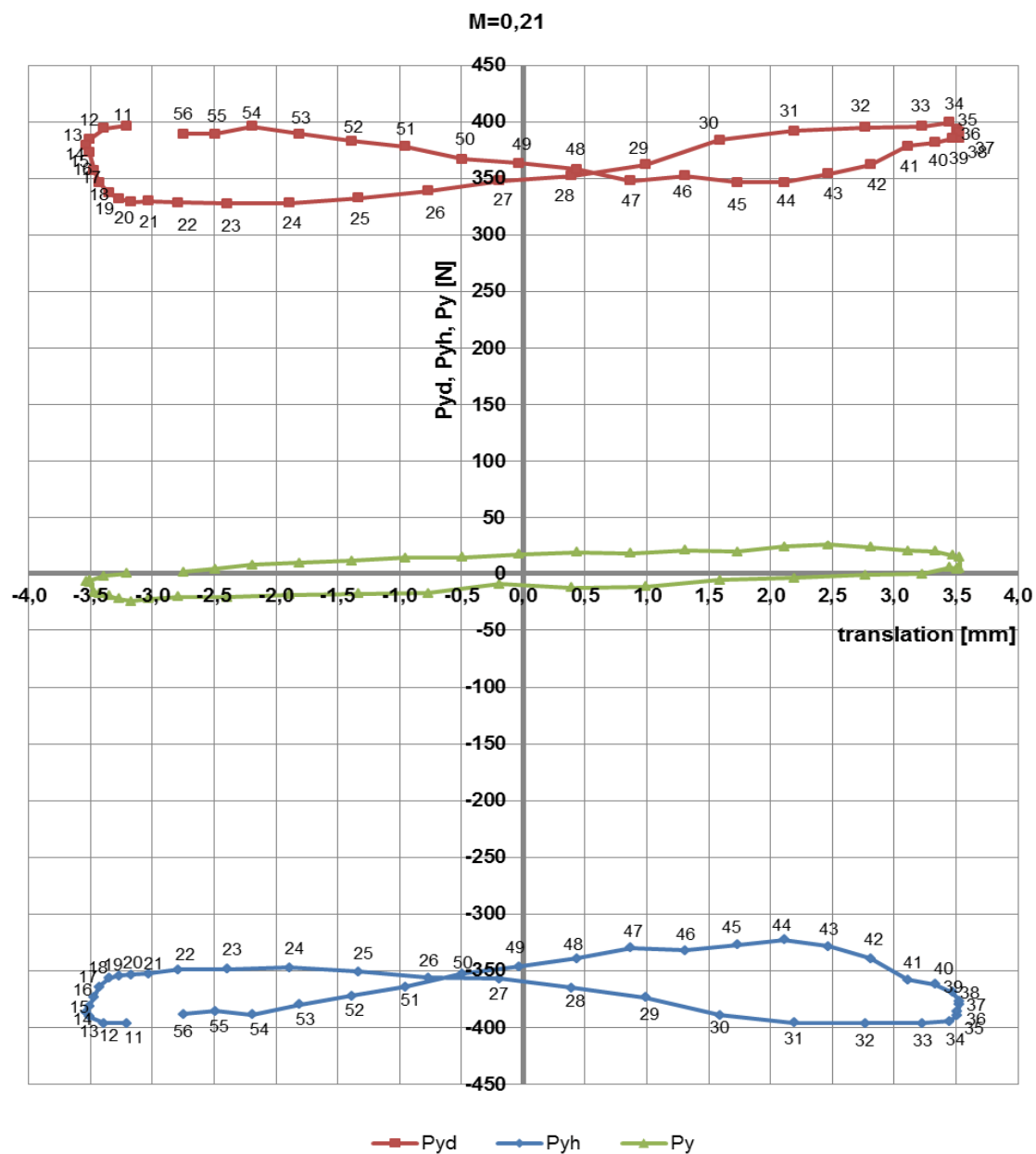
Fig. 8b Total lifting force as a function of profile translation ($M = 0.45$)

There are two types of cycles depicted in Fig. 9a and Fig. 9b for $M = 0.21$ and $M = 0.45$, respectively. Flutter regime (see also interferogram Fig. 2a, $M = 0.21$):

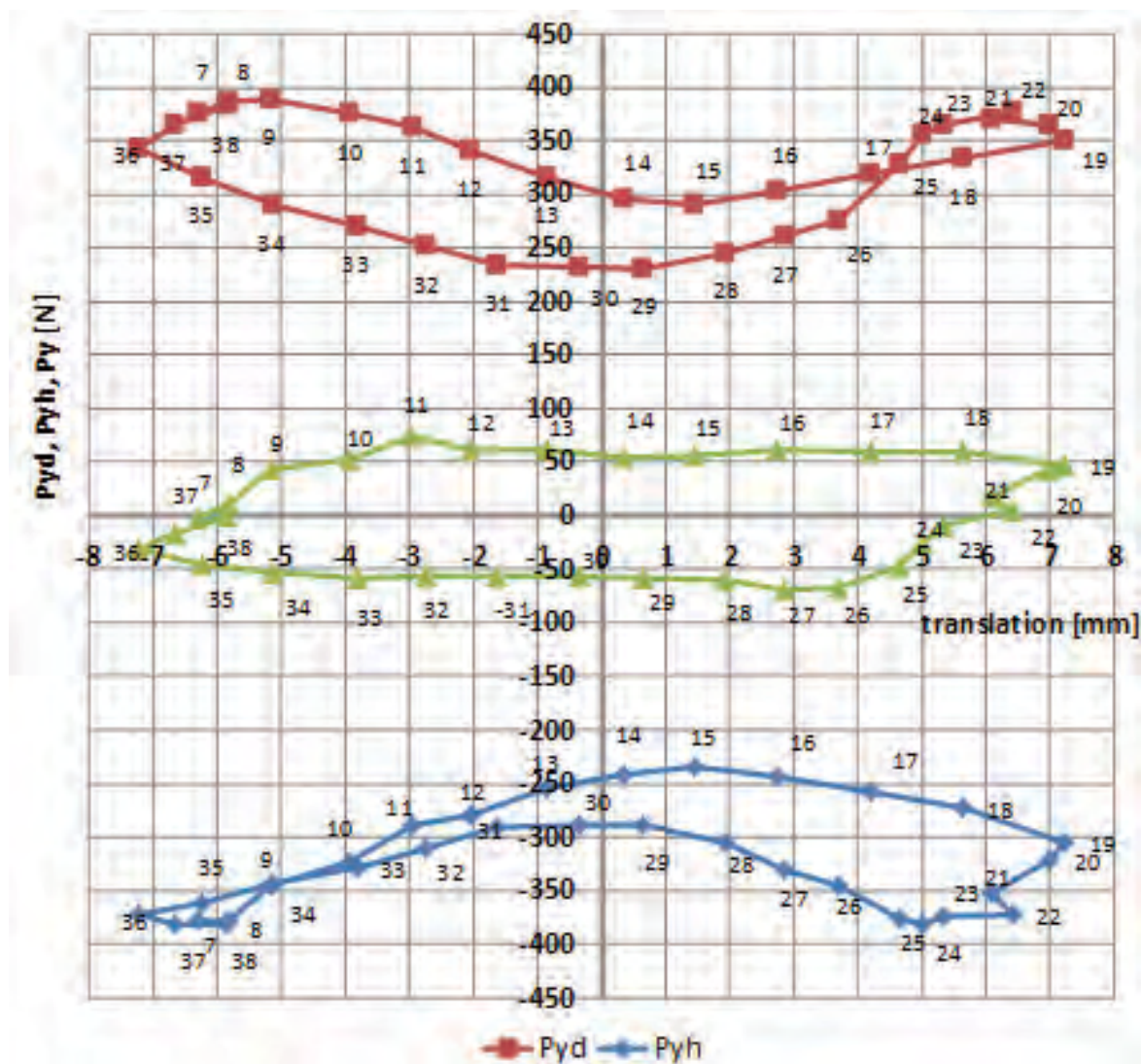
- The elliptical curve situated in the middle of the figure represents the cycle with negative (counterclockwise) rotation, see Fig. 8a,
- In the upper and lower part of the diagram there are trajectory loops – the additive components of the middle elliptical curve. These loops are going in the same sense and represent variable forces existing separately on the upper and lower surfaces. The forces are interconnected by means of the circulation.

Stall flutter regime (see also interferogram Fig. 2b, $M = 0.45$):

- The elliptical curve situated in the middle of the figure represents the cycle with positive (clockwise) rotation (see Fig. 8b),
- Loops in the upper and lower part of the diagram are going in opposite sense.



Obr. 9a The lift as the function of the translation ($M = 0.21$, P_{yd} – lower, P_{yh} – upper surface).



Obr. 9b The lift as the function of the translation ($M = 0.45$, P_{yd} – lower, P_{yh} – upper surface).

3. Conclusions

The interferometric measurements of unsteady aerodynamic forces acting on the profile NACA 0015 surface were evaluated during one period of flutter vibration, for the flow velocity $M = 0.21$ and $M = 0.45$. The decomposition of the lifting forces into two parts (loading the upper and lower surfaces) enables to obtain original results that describe the dynamical behaviour of the system after the loss of aeroelastic system stability in the flutter and stall-flutter regime.

Acknowledgement

The authors gratefully acknowledge the Grant Agency of the Czech Republic for supporting this work under Grant No. 13-10527S „Subsonic flutter analysis of elastically supported airfoils using interferometry and CFD“.

References

Vlček, V., Kozánek, J., Zolotarev, I. (2013) Optical measurement of the flow field around the aerodynamic profile in flutter regime. *Proc. Colloquium Dynamics of Machines 2013*, Institute of Thermomechanics AS CR, v.v.i., Prague, 2013, pp. 131-138, (in Czech).